

A novel view of plane wave expansion method in photonic crystals

Young-Chung Hsue* and Tzong-Jer Yang†

Department of Electrophysics, National Chiao-Tung University, Hsinchu, Taiwan, Republic of China

(Dated: March 19, 2018)

We propose a method derived from the simple plane wave expansion that can easily solve the interface problem between vacuum and a semi-infinite photonic crystal. The method is designed to find the complete set of all the eigenfunctions, propagating or evanescent, of the translation operators $\{\mathbf{T}_\mathbf{R}\}$, at a fixed frequency. With these eigenfunctions and their eigenvalues, the transmitted and reflected waves can be determined. Two kinds of applications are presented for 2D photonic crystals. The first is a selection rule for determine the normal direction of the vacuum-photonic crystal interface to achieve the highest attenuation effect at a gap frequency. The second is to calculate the transmittance and reflectance for a light incident from vacuum to an semi-infinite photonic crystal. As an example we recalculate a system studied previously by K. Sakoda et al. and get results in agreement with theirs.

PACS numbers: 42.70.Qs, 85.60.Bt

Since Yablonovitch [1, 2, 3] discovered a periodic dielectric structure that has an absolute gap in the frequency spectrum for electromagnetic waves, the idea of photonic crystals have attracted great interest. Many phenomena have been predicted theoretically and many application possibilities have been explored [2, 4, 5, 6]. Corresponding studies in the early years most authors paid their attention on the frequency spectrum gaps, and the most convenient method to calculate the band gaps is the plane wave expansion method [7, 8]. Recently, various kinds new methods have been proposed to compute some other relevant physical parameters such as transmittance and penetration depth [9, 10, 11, 12] for a finite system.

In this paper we also address the transmittance and penetration depth problems, but use a different method that includes all the information of propagating and evanescent modes getting from the translation operator. We show that by appropriately modifying the conventional plane wave expansion method we can enlarge its application region, and which makes it easy to solve the interface problem between vacuum and a semi-infinite photonic crystal system.

Our method has several advantages. First, both the “air rods in dielectric” and “dielectric rods in air” problems can be solved, without any restriction on the shapes of the rods and position of cutting plane that separating the semi-infinite photonic crystal region from the air region, which is impossible for the LKKR method [14, 15, 16, 17, 18]. Second, all information getting from the complete set of the eigenfunctions of the translation operator are used, including both the propagating and evanescent modes. This makes it easy to analyze and discuss phenomena using the well established knowledge of solid state physics. Third, the finite size effects such as

the resonance behavior of the transmittance curve caused by the finite thickness of the photonic crystal sample can be easily isolated. We can thus accurately calculate the transmittance and reflectance for a very thick photonic crystal sample.

For a system without free charge and current, and if the permittivity $\epsilon(\mathbf{r})$ and permeability $\mu(\mathbf{r})$ are scalars independent of time, the magnetic field $\mathbf{H}(\mathbf{r}, t)$ satisfies

$$\nabla \times \frac{1}{\epsilon} \nabla \times \mathbf{H}(\mathbf{r}, t) = -\mu \frac{\partial^2}{\partial t^2} \mathbf{H}(\mathbf{r}, t), \quad (1)$$

where $\mathbf{H}(\mathbf{r}, t) = \sum_{\omega} \mathbf{H}_{\omega}(\mathbf{r}) e^{-i\omega t}$, and

$$\nabla \times \frac{1}{\epsilon} \nabla \times \mathbf{H}_{\omega}(\mathbf{r}) = \mu \omega^2 \mathbf{H}_{\omega}(\mathbf{r}). \quad (2)$$

In addition, if $\epsilon(\mathbf{r})$ and $\mu(\mathbf{r})$ are periodic functions, following the derivation of Bloch theory, Eq. (2) can be changed to

$$\begin{aligned} - \sum_{\mathbf{G}'} (\mathbf{k} + \mathbf{G}) \times \epsilon_{\mathbf{G}-\mathbf{G}'}^{-1} (\mathbf{k} + \mathbf{G}') \times \mathbf{H}_{\mathbf{k}, \mathbf{G}'} \\ = \omega^2 \sum_{\mathbf{G}'} \mu_{\mathbf{G}-\mathbf{G}'} \mathbf{H}_{\mathbf{k}, \mathbf{G}'}, \end{aligned} \quad (3)$$

where $\mathbf{H}_{\omega}(\mathbf{r}) = \sum_{\mathbf{G}} e^{i(\mathbf{k}+\mathbf{G})\cdot\mathbf{r}} \mathbf{H}_{\mathbf{k}, \mathbf{G}}$, $\epsilon(\mathbf{r}) = \sum_{\mathbf{G}} e^{i\mathbf{G}\cdot\mathbf{r}} \epsilon_{\mathbf{G}}$, $\mu(\mathbf{r}) = \sum_{\mathbf{G}} e^{i\mathbf{G}\cdot\mathbf{r}} \mu_{\mathbf{G}}$, and $\{\mathbf{G}\}$ is the set of the reciprocal lattice. Since in this paper we consider only two-dimensional cases, we have $k_z = 0$, and the electromagnetic waves can be decoupled as E polarization (TE) and H polarization (TM) modes. For example, the TM mode of \mathbf{H} field is written as $\mathbf{H} = H_z \hat{z}$ and satisfy

$$\begin{aligned} \sum_{\mathbf{G}'} \epsilon_{\mathbf{G}-\mathbf{G}'}^{-1} (\mathbf{k} + \mathbf{G}) \cdot (\mathbf{k} + \mathbf{G}') H_{z, \mathbf{k}, \mathbf{G}'} \\ = \omega^2 \sum_{\mathbf{G}'} \mu_{\mathbf{G}-\mathbf{G}'} H_{z, \mathbf{k}, \mathbf{G}'}. \end{aligned} \quad (4)$$

*Electronic address: ychsue.ep87g@nctu.edu.tw

†Electronic address: yangtj@cc.nctu.edu.tw

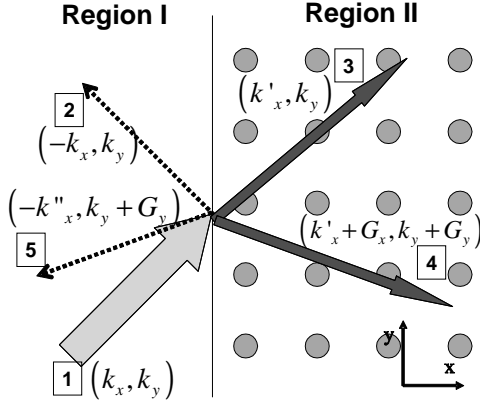


FIG. 1: A schematic view of the light incident from region I to region II, where region I is vacuum and region II is PC. The gray, dotted, and black arrows represent the incident, reflected, and transmitted light, respectively. For the incident light, $\mathbf{k} = (k_x, k_y)$. According to Bloch theory, the modes of region II can be written as $H_z(\mathbf{r}) = \sum_{\mathbf{G}} H_{\mathbf{G}} e^{i(\mathbf{k}' + \mathbf{G}) \cdot \mathbf{r}}$. Based on the continuity conditions at the interface, reflection and transmission modes have $\mathbf{k}_{ref} = (-k''_x, k_y + G_y)$ and $\mathbf{k}_{trans} = (k'_x + G_x, k_y + G_y)$, where $k''_x = \sqrt{\frac{\omega^2}{c^2} - (k_y + G_y)^2}$, and k'_x 's are obtained from solving Eq. (6).

Conventionally, treating Eq. (4) as an eigenvalue problem, the propagating bulk modes of an infinite periodic system for a given real \mathbf{k} can be obtained straightforwardly. However, in most of the situations we also need to know the transmittance and reflectance of a finite or semi-infinite system for an incident light. In order to obtain these quantities, various methods such like LKKR [10, 12, 13], transfer matrix [14, 15, 16, 17], and scattering matrix [18] method have been proposed. In these kinds of methods, a photonic crystal slab is treated as the stack of many gratings. The matrix problem for only one

grating layer is solved first, then multiplying the matrices layer by layer and the total transmittance and reflectance can be determined. Although these methods are successful, however, in order to confirm the good numerical accuracy, the number of layers should be restricted to a small value. In addition, using these methods it is hard to find the relations between the transmittance and the original band structure.

In this paper, we propose an alternative method to calculate the transmitted and reflected waves from the interface between vacuum and a semi-infinite photonic crystal for an incident plane wave. The method is based on Eq. (4), which contains all the information of the band structure of the system. We thus can easily analyze the physical meanings of various phenomena using the knowledge getting from the solid state physics.

Here, if the k_x and k_y are fixed, the frequency ω can be solved as an eigenvalue problem. If the system is infinitely extended, there are just only propagation modes that can survive. However, sometimes we have to calculate the transmission and reflection coefficients for a finite sized or semi-infinite sample, which have at least one boundary. At the edges of the sample, the periodic structure is broken and the evanescent modes must be considered. However, it is impossible to obtain the evanescent solutions from the eigenvalue problem of Eq. (4) because it provides the solutions for an extended bulk and the boundary conditions at infinite restrict the k_x and k_y to be taken as real values.

Nevertheless, can we make some modifications to produce the attenuated solutions of Eq. (4)? The answer is yes. For different purposes, there are two kinds of calculations: one is to fix the direction of \mathbf{k} and frequency; the other is to fix k_y and frequency. With a simple transformation, the Eq. (4) can be rewritten as

$$\begin{pmatrix} 0 & \hat{\mathbf{I}} \\ \epsilon_{\mathbf{G}-\mathbf{G}''} [\omega^2 \mu_{\mathbf{G}''-\mathbf{G}'} - \epsilon_{\mathbf{G}''-\mathbf{G}'}^{-1} \mathbf{G}'' \cdot \mathbf{G}'] & -\epsilon_{\mathbf{G}-\mathbf{G}'} [\epsilon_{\mathbf{G}''-\mathbf{G}'}^{-1} \hat{\mathbf{k}} \cdot (\mathbf{G}'' + \mathbf{G}')] \end{pmatrix} \begin{pmatrix} H_{\mathbf{G}'} \\ k H_{\mathbf{G}'} \end{pmatrix} = k \begin{pmatrix} H_{\mathbf{G}'} \\ k H_{\mathbf{G}'} \end{pmatrix} \quad (5)$$

for fixed direction and frequency, where (respectively) $H_{\mathbf{G}'}$, $\hat{\mathbf{I}}$ and $\hat{\mathbf{k}}$ denote the abbreviation of $H_{z,\mathbf{k},\mathbf{G}'}$, $\delta_{\mathbf{G},\mathbf{G}'}$ and unit vector of \mathbf{k} , and

$$\begin{pmatrix} 0 & \hat{\mathbf{I}} \\ \epsilon_{\mathbf{G}-\mathbf{G}''} [\omega^2 \mu_{\mathbf{G}''-\mathbf{G}'} - \epsilon_{\mathbf{G}''-\mathbf{G}'}^{-1} (\mathbf{G}'' + k_y \hat{\mathbf{y}}) \cdot (\mathbf{G}' + k_y \hat{\mathbf{y}})] & \hat{\mathbf{P}} \end{pmatrix} \begin{pmatrix} H_{\mathbf{G}'} \\ k_x H_{\mathbf{G}'} \end{pmatrix} = k_x \begin{pmatrix} H_{\mathbf{G}'} \\ k_x H_{\mathbf{G}'} \end{pmatrix} \quad (6)$$

for fixed k_y and frequency, where $\hat{\mathbf{y}}$ and $\hat{\mathbf{P}}$ denote unit vector of y direction and $-\epsilon_{\mathbf{G}-\mathbf{G}''} [\epsilon_{\mathbf{G}''-\mathbf{G}'}^{-1} (\mathbf{G}''_x + \mathbf{G}'_x)]$, respectively. If the \mathbf{k} and \mathbf{G} in Eq. (5) are acted by a rotation operator $\hat{\Theta}$ which rotates $\hat{\mathbf{k}}$ to x -direction — i.e. $\hat{\Theta} \hat{\mathbf{k}} = \hat{\mathbf{x}}$ — and we define $\tilde{\mathbf{G}} \equiv \hat{\Theta} \mathbf{G}$, then Eq. (5)

becomes Eq. (6) in which $\tilde{\mathbf{G}}$ is substituted for \mathbf{G} and $k_y = 0$. Following this cue, the Eq. (5) can be considered as a master equation for solving a problem where the incident light is always perpendicular to the interface. From which we can easily determine the penetration depth along direction $\hat{\mathbf{k}}$. If our purpose is to use the

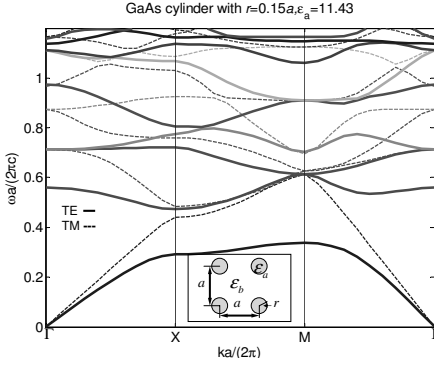


FIG. 2: The frequency spectrum of the square lattice photonic crystal is derived from Eq. (4). In this figure, solid lines and dash lines denote the TE and TM modes, respectively.

$$\begin{pmatrix} -\langle x_0 y | H_m^I \rangle & \langle x_0 y | H_m^{II} \rangle \\ -\langle x_0 y | \epsilon^{-1} \partial_x | H_m^I \rangle & \langle x_0 y | \epsilon^{-1} \partial_x | H_m^{II} \rangle \end{pmatrix} \begin{pmatrix} \langle H_m^I | \hat{\mathbf{R}} | H_0^I \rangle \\ \langle H_m^{II} | \hat{\mathbf{T}} | H_0^I \rangle \end{pmatrix} = \begin{pmatrix} \langle x_0 y | H_0^I \rangle \\ \langle x_0 y | \epsilon^{-1} \partial_x | H_0^I \rangle \end{pmatrix}, \quad (7)$$

where $\hat{\mathbf{R}}$ and $\hat{\mathbf{T}}$ are the reflection and transmission operators, H_m^I and H_m^{II} are the reflection modes in region I and transmission modes in region II, the m denotes the different modes, respectively. And H_0^I is the incident light.

If Eq. (7) is expanded in K-space, it can be rewritten as

$$\hat{\mathbf{A}} \begin{pmatrix} \langle H_{Im} | \hat{\mathbf{R}} | H_{I0} \rangle \\ \langle H_{IIIm} | \hat{\mathbf{T}} | H_{I0} \rangle \end{pmatrix} = \begin{pmatrix} H_{z,\mathbf{k},G_y}^{I,i} \\ k_{G_y,x}^{I,i} H_{z,\mathbf{k},G_y}^{I,i} \end{pmatrix}, \quad (8)$$

where

$$\hat{\mathbf{A}} = \begin{pmatrix} -H_{z,\mathbf{k},G_y}^{I,r} & \sum_{G_x} H_{z,\mathbf{k},\mathbf{G}}^{II,t} \\ -k_{mx}^{I,r} H_{z,\mathbf{k},G_y}^{I,r} & \sum_{G_x, G'} \epsilon_{\mathbf{G}-\mathbf{G}'}^{-1} (k_{mx}^{II} + G'_x) H_{z,\mathbf{k},\mathbf{G}}^{II,t} \end{pmatrix},$$

and $H_{z,\mathbf{k},\mathbf{G}}$ can be gotten from Eq. (6), and i, r and t denote incident, reflection and transmission, respectively. To determine the transmission and reflection coefficients, we have to first decide the direction of the Poynting vector of every mode. For \mathbf{k} is a real vector, it can either be obtained from $\mathbf{v}_g = \vec{\nabla}_{\mathbf{k}} \omega$ or from

$$\begin{aligned} & \int_{cell} \text{Re} \left\{ -\frac{i}{\omega \epsilon} H_z^* \vec{\nabla} H_z \right\} dr^2 \\ & = \sum_{\mathbf{G}, \mathbf{G}'} \text{Re} \left\{ \frac{1}{\omega} H_{z,\mathbf{k},\mathbf{G}}^* \epsilon_{\mathbf{G}-\mathbf{G}'}^{-1} (\mathbf{k} + \mathbf{G}') H_{z,\mathbf{k},\mathbf{G}'} \right\} \end{aligned} \quad (9)$$

For \mathbf{k} is a complex number, propagation toward right hand side corresponds to $\text{Im}(k_x) > 0$. When group velocity

band gap effect of the structure, then the result obtained from this calculation will tell us how to cut the sample to get the highest performance.

On the other hand, Eq. (6) can be used to deal with the problem for light incident with different angle θ , which is the angle between the normal vector of the interface and \mathbf{k} of the incident light. Here $\tan \theta = k_y / \sqrt{\omega^2/c^2 - k_y^2}$. Figure 1 explains the details.

Since we can obtain all the eigenvectors of the system, the transmission and reflection spectra can also be obtained. Based on the continuity conditions at the interface, the relationship between the \mathbf{H} fields in region I and region II can be written as

locity and $H_{z,\mathbf{k},\mathbf{G}}$ of each mode are known, the transmittance \mathbf{T} and reflectance \mathbf{R} can be gotten from them, and the accuracy can be estimated from how $\mathbf{R} + \mathbf{T}$ is close to one. Sometimes, $\det[\mathbf{A}]$ is possible to become zero, if so, the Eq. (8) has nonzero solutions when there is no incident light. This kind of wave is a surface state which resembles the surface plasmon propagating along the surface of a metal. However, we do not discuss it in this paper. One more interesting thing among these three equations — from Eq.(4) to Eq.(6) — is that they are identical to each other. Because the second row of matrices of left side of Eq. (5) and Eq. (6) are equal to Eq. (4) while the $\{\mathbf{G}\}$ in these equations are equal. Thus any eigenfunction of one of these three equations satisfies another two equations. It leads to two useful things: (i) the real \mathbf{k} contours of these three methods with equal frequency are the same. (ii) The $\{\mathbf{G}\}$ needn't to be changed when these three equations are considered as a series of policy tools. For example, we should decide where the band edge is and select the ω_0 near the band edge to obtain the band structure from Eq. (4) if we hope to observe what happened near the band gap. By replacing the frequencies of Eq. (5) and (6) by ω_0 , the penetration depth can be derived from Eq. (5) and so do the variations of transmittance while the solutions of Eq. (6) are used in Eq. (7). During this process, even if we just select $\mathbf{G} = 0$ and drop out $\mathbf{G} \neq 0$ for average assumption in the calculations of Eq. (4), the $\{\mathbf{G}\}$ still needn't to be changed in the following calculations.

For simplicity, the structure we used in obtaining Fig. 2 and Fig. 3 is the square lattice with GaAs ($\epsilon = 11.43$) cylinders each with radius $= 0.15a$ inside vacuum; whereas

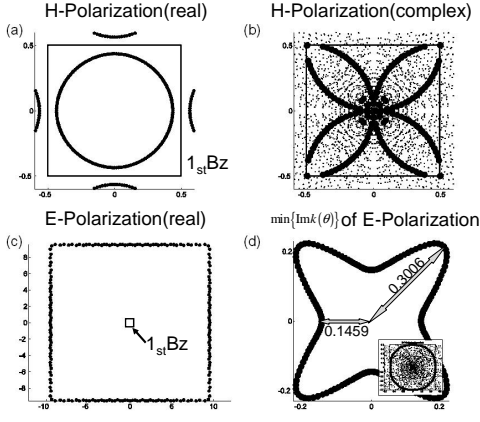


FIG. 3: Possible \mathbf{k} values for a constant-frequency $\omega = 0.4$. The solid square frames in these figures are the first Brillouin zone boundaries and the data taken are inside the first Brillouin zone. (a) and (b) are for the TM waves (H-polarization), (c) and (d) are for the TE waves (E-polarization). (a) and (c) are constant-frequency contours (with purely real \mathbf{k}) of propagating waves. (b) and the inset of (d) show the contours of $\text{Re}\{\mathbf{k}\}$ of evanescent modes. In addition, (d) shows the $\min\{\text{Im} k(\theta)\}$. The spots in the (b) and the inset of (d) correspond to the cases with smallest $\text{Im}(\mathbf{k})$ or longest penetration depth.

in Fig. 4 we employ vacuum cylinders each with radius $0.43077a$ inside the $\text{PbO}(\epsilon = 2.72)$ background. In all cases, a is the lattice constant and the primitive vectors are given by $\mathbf{a}_1 = (a, 0)$ and $\mathbf{a}_2 = (0, a)$.

The first application is a selection rule to determine the interface direction for the highest performance of light insulation. We solve Eq. (5) at a frequency equal to $0.4(2\pi c/a)$ and the results are presented in Fig. 3. In Fig. 2, there is a band gap at $\omega = 0.4(2\pi c/a)$ for the TE mode, so that in Fig. 3(c), there are no real number solutions inside the first Brillouin zone. However, outside and far away from the 1st Brillouin zone such solutions exist, which are fake and are caused by the finite basis used in the calculations. To find the interface direction we first choose a direction $\hat{\mathbf{k}}$ and use Eq. (5) to find a k that has the smallest $|\text{Im}(k)|$ value, which denoted as $k_I(\theta)$ and determines the main decay trend for a wave propagating along $\hat{\mathbf{k}}$. The second step is to scan angles from 0° to 45° to find an angle θ_0 that has the maximum $k_I(\theta)$. The details are shown in Fig. 3(d), where we calculate the TE modes, and the penetration depths (i.e., $2\pi/k_I(\theta)$) for 0° and 45° are $6.8540a$ and $3.3272a$, respectively. This indicates that when we produce a sample that cut along 45° , it just needs 4 or 5 layers to stop the light with $\omega = 0.4(2\pi c/a)$ for TE modes instead of 7 or 8 layers for 0° .

The second application is to fix k_y and frequency in order to obtain k_x . For comparison, we select the system discussed in [9] to contrast with our system and show the result in Fig. 4. The system in [9] is a 16 layers photonic crystal which is a square lattice (with a lattice constant

a) of air columns (radius equals $0.43077a$ and is located at the center of a unit cell) in a dielectric substrate PbO placed in air and our system is a semi-infinite photonic crystal placed in air. By using Eq. (6) and Eq. (8) the transmittance can be obtained as shown in Fig. 4. Because our system is infinite, we can find something quite different.

(1) The solid lines and dashed lines are almost smooth curves except in the gap regime and at some special points ($\omega = 0.74$ and 0.85 in TE mode). The oscillating solid lines with dots in Fig. 4 represent the solutions of [9]. It is obvious that our curves are different from that of [9]. The oscillation behavior is owing to finite thickness. They can be easily explained by a roughly consideration of the average dielectric $\bar{\epsilon} \equiv \langle \epsilon \rangle_{\text{cell}}$. For low frequency, the most important contribution of $\epsilon_{\mathbf{G}}$ is $\epsilon_{\mathbf{G}=0}$, which is equal to $\bar{\epsilon}$, therefore the 16 layers photonic crystals can be considered as an effective material with uniform dielectric $\bar{\epsilon} = 1.7173\epsilon_0$ and width $16a$, where a is the lattice constant of the photonic crystal and ϵ_0 is the permittivity of free space. This is a typical 1D problem and the waves in both sides of this material can be connected by transfer matrix whose formula is

$$\mathbf{M}_\omega \begin{pmatrix} e^{ik16a} & 0 \\ 0 & e^{-ik16a} \end{pmatrix} \mathbf{M}_\omega^{-1},$$

where \mathbf{M}_ω is a 2×2 matrix with $\det |\mathbf{M}_\omega| \neq 0$ determined by the optical impedance contrast and the incident angle, and $k = \omega\sqrt{\bar{\epsilon}\mu_0}$ is the effective wave number, where μ_0 is permeability of free space. It is obvious that the transfer matrices equals $\pm \mathbf{I}$ when $k16a = n\pi$, where n is an integer number. That means the frequency difference between two neighboring peaks is

$$\Delta\tilde{\omega} = \frac{1}{32\sqrt{\bar{\epsilon}/\epsilon_0}} = \frac{1}{32\sqrt{1.7173}} \simeq 0.0238,$$

where $\tilde{\omega} = \frac{\omega a}{2\pi c}$. Comparing with the average width 0.0222 of peaks between $\frac{\omega a}{2\pi c} = 0.5$ to 0.7 , we can say the oscillation in Fig. 4 comes from the effect of finite size.

(2) In the vicinity of $\tilde{\omega} \simeq 0.74$, according to the band structure calculation results the spectrum should ascend rapidly when $\tilde{\omega}$ is increasing, because it is at band edge. But, the real situation appears in Fig. 4(a) is ascending quickly and descending immediately to near zero transmittance. Our explanation is that there are two propagation mode's with group velocity $v_g \simeq 0$, so they do not contribute to the transmittance.

(3) In Fig. 4(a), the valley of transmittance near $\omega = 0.85$ disappears when the interface is chosen to pass through the center of the vacuum cylinders. This reveals that it is possible to stop the light at some isolated frequency points by appropriately choosing the cutting plane of the photonic crystal even if the frequencies are outside of band gaps.

(4) In Fig. 4(b), there should be a forbidden band for $\omega = 0.75$ to 0.78 , but the line with dots does not show

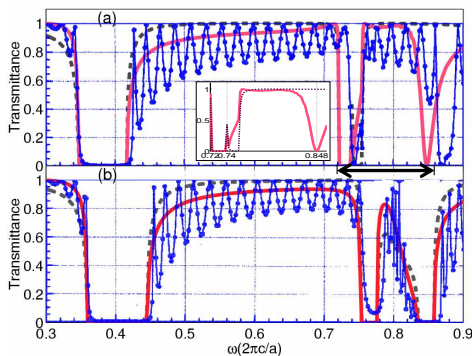


FIG. 4: Transmittance of the (a) TE and (b) TM modes. The line with dots is the data excerpted from Ref. [9]. The solid lines and dashed lines are our solutions with different cut planes (in the solid line case the cut plane is the same as in [9], whereas in the dashed line case the cut plane passes through the centers of the cylindrical holes), and the inset is the clearer view of (a) whose frequency regime is indicated by \leftrightarrow .

this result. According our calculation the wave attenuation rate for a 16-layer structure is about 0.0733, which agrees with the result shown by the line with dots. This phenomenon shows that the evanescent modes do contribute the transmittance in a finite thickness structure.

In these two applications, the evanescent modes are necessary and useful for the calculations of semi-infinite system, and this method also provides us some informa-

tion such like for how large a separation distance between two defects can they be treated as independent in super-cell method.

In conclusion, the method we present here may not be efficient enough, because in the calculation we get results both inside and outside of the first Brillouin zone (FBZ). However, only the results inside the FBZ are useful and the others repeat the same information and are redundant. For example, if we use N^2 bases, there are only $2N$ useful eigenfunctions. Besides, this method has several advantages. First, from this method we can easily realize and analyze some properties of periodic systems with interface and the computational time is independent of the number of layers. Thus, even if the number of layers is very large, it will save much time. Second, using Eq. (9), we can also calculate the density of states, $D(\omega)$, through

$$D(\omega) = \int_{shell} \frac{dk_{//}}{|\nabla_{\mathbf{k}}\omega|}. \quad (10)$$

They are especially useful when we aim to calculate the density of states in some small frequency regimes.

We are now investigating the cases of finite size specimens and a structure with line defects.

Finally, we thank Prof. B. Y. Gu for instructing us about Andreev reflection, which gave us a chance to employ this idea about Eq. (5), and thank Dr. P. G. Luan who let us find more possibilities with this method.

-
- [1] E. Yablonovitch, Phys. Rev. Lett. 58, 2055 (1987)
 - [2] E. Yablonovitch, T. J. Gmitter, Phys. Rev. Lett. 67, 3380 (1991)
 - [3] E. Yablonovitch, T. J. Gmitter, and K. M. Leung, Phys. Rev. Lett. 67, 2295 (1991)
 - [4] G. Kurizki and A. Z. Genack, Phys. Rev. Lett. 61, 2269 (1988).
 - [5] S. John and J. Wang, Phys. Rev. B 43, 12772 (1991).
 - [6] S. L. McCall, P. M. Platzman, R. Dalichaouch, D. Smith, and S. Schultz, Phys. Rev. Lett. 67, 2017 (1991).
 - [7] K. Sakoda, *Optical Properties of Photonic Crystals* (Springer-Verlag, 2001).
 - [8] Z. Y. Li, B. Y. Gu, and G. Z. Yang, Phys. Rev. Lett. 81, 2574 (1998); Eur. Phys. J. B 11, 65 (1999).
 - [9] K. Sakoda, Phys. Rev. B 52, 8992 (1995)
 - [10] J. B. Pendry, J. Mod. Opt. 41, 209 (1994)
 - [11] B. Gralak, S. Enoch and G. Tayeb, J. Opt. Soc. Am. A 17, 1012-1020 (2000).
 - [12] J. B. Pendry and A. MacKinnon, Phys. Rev. Lett. 69, 2772 (1992)
 - [13] J. B. Pendry, J. Phys. Cond. Matt. 8, 1085-1108 (1996).
 - [14] N. Stefanou, V. Karathanos, and A. Modinos, J. Phys. Cond. Matt. 4, 7389-7400 (1992).
 - [15] V. Yannopapas, N. Stefanou, and A. Modinos, J. Phys. Cond. Matt. 9, 10261-10270 (1997).
 - [16] N. Stefanou, V. Yannopapas, and A. Modinos, Comput. Phys. Commun. 132, 189-196 (2000).
 - [17] K. Ohtaka, Phys. Rev. B 19, 5057 (1979); J. Phys. C 13, 667 (1980); A. Modinos, Physica A 141, 575 (1987).
 - [18] L. C. Botten, Phys. Rev. E 64, 046603 (2001)